Supplementary information

Self-assembled, bivalent aptamers on graphene oxide as an efficient anticoagulant

Pei-Xin Lai,[a] Ju-Yi Mao,[a,b,c] Binesh Unnikrishnan,[a] Han-Wei Chu,[a] Chien-Wei Wu,[d] Huan-Tsung Chang,[d,e] and Chih-Ching Huang*[a,f,g]

[a]Department of Bioscience and Biotechnology, National Taiwan Ocean University, Keelung 20224, Taiwan

[b]Doctoral Degree Program in Marine Biotechnology, National Taiwan Ocean University, Keelung 20224, Taiwan

[c]Doctoral Degree Program in Marine Biotechnology, Academia Sinica, Taipei 11529, Taiwan

[d]Department of Chemistry, National Taiwan University, Taipei 10617, Taiwan

[e]Department of Chemistry, Chung Yuan Christian University, Taoyuan City 32023, Taiwan

[f]Center of Excellence for the Oceans, National Taiwan Ocean University, Keelung 20224, Taiwan

[g]School of Pharmacy, College of Pharmacy, Kaohsiung Medical University, Kaohsiung, 80708, Taiwan

Correspondence: Professor Chih-Ching Huang, Department of Bioscience and Biotechnology, National Taiwan Ocean University, 2 Pei-Ning Road, Keelung 20224, Taiwan; Tel.: 011-886-2-2462-2192 ext. 5524; Fax: 011-886-2-2462-2320; E-mail: huanging@ntou.edu.tw

Table S1. DNA sequences of the TBAs used in this study.

Name	Sequence[a]
$TBA_{15}h_{20}A_{20}$	**5′-TCA GTG GGG TTG GTG TGG TTG GTG CCT GAT TTT TCA ATA GAG TCG TAC AGG TCG AAA AAA AAA AAA AAA AAA AA-3′**
$TBA_{29}h_{20}A_{20}$	**5′-AAA AAA AAA AAA AAA AAA AAC GAC CTG TAC GAC TCT ATT GTT TTT AGT CCG TGG TAG GGC AGG TTG GGG TGA CT-3′**

[a]underline indicates hybrid pairs

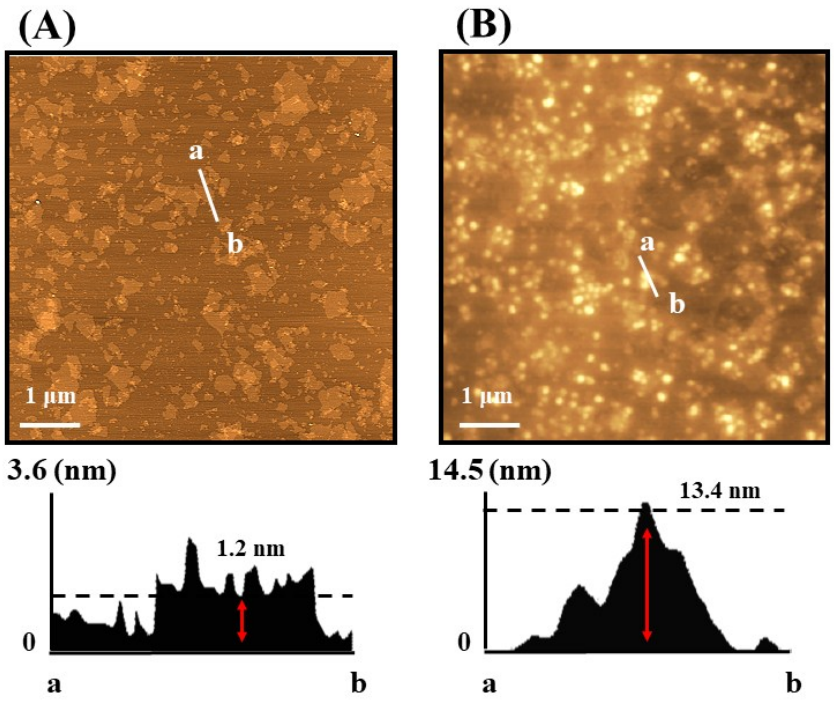

Figure S1. Tapping mode AFM images of (A) GO and (B) TBA_{15}/TBA_{29}–GO.

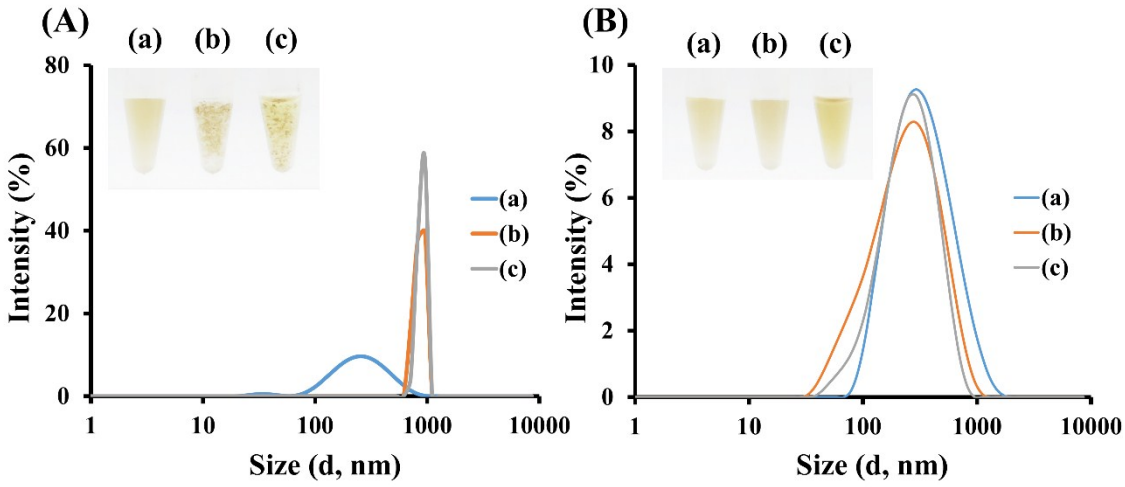

(C)

	sample	Hydrodynamic Radius (Rh)	polydispersity index (PDI)
GO	(a)	~110 nm	0.312
	(b)	~495 nm	0.562
	(c)	~477 nm	0.477
TBA_{15}/TBA_{29}–GO	(a)	~124 nm	0.281
	(b)	~120 nm	0.295
	(c)	~121 nm	0.284

Figure S2. Dynamic light scattering (DLS) spectra of (A) GO and (B) TBA_{15}/TBA_{29}–GO in (a) sodium phosphate buffer solution (5.0 mM, pH 7.4), (b) PBS solution, and (c) two-fold diluted plasma solution. (C) Hydrodynamic radius (Rh) and polydispersity index of GO and TBA_{15}/TBA_{29}–GO in various conditions. Insets in (A) and (B): photographic images of the corresponding solutions. The concentrations of GO and TBA_{15}/TBA_{29}–GO for the photography and DLS measurements are 8 μg mL^{-1} (in terms of GO).

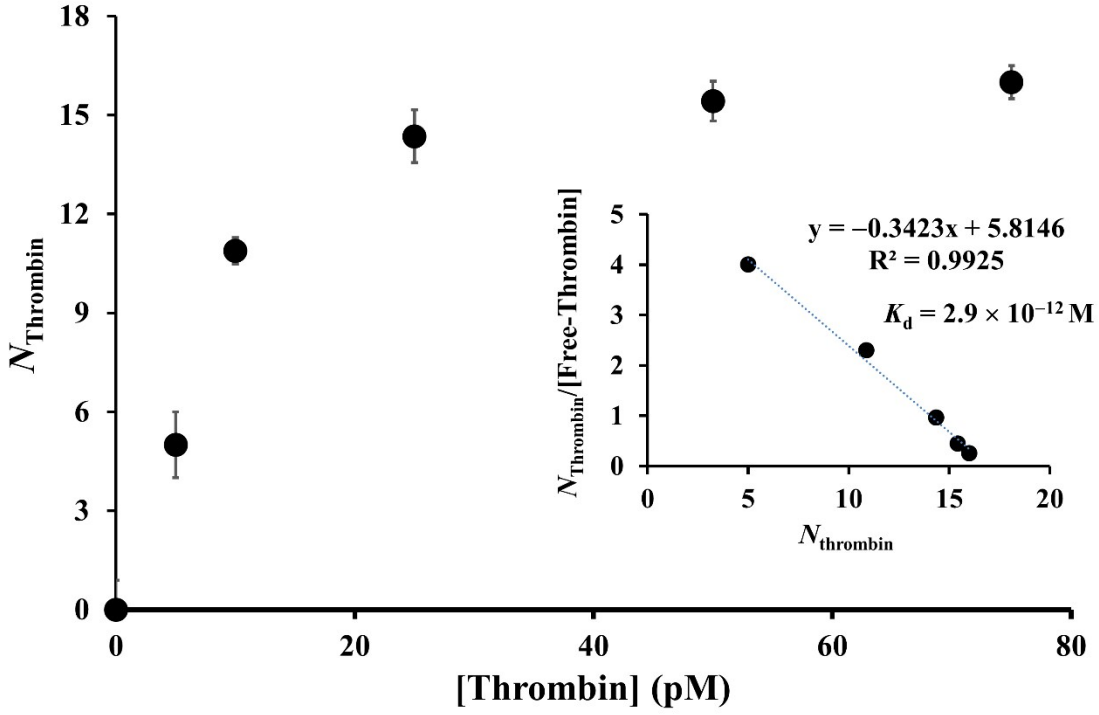

Figure S3. Plots for calculating the dissociation constant, K_d, for thrombin and TBA_{15}/TBA_{29}–GO. $N_{thrombin}$ is the concentration of thrombin bound to TBA_{15}/TBA_{29}–GO at equilibrium, and [Free–Thrombin] is the free thrombin concentration at equilibrium. Error bars represent the standard deviations of experiments in triplicate.

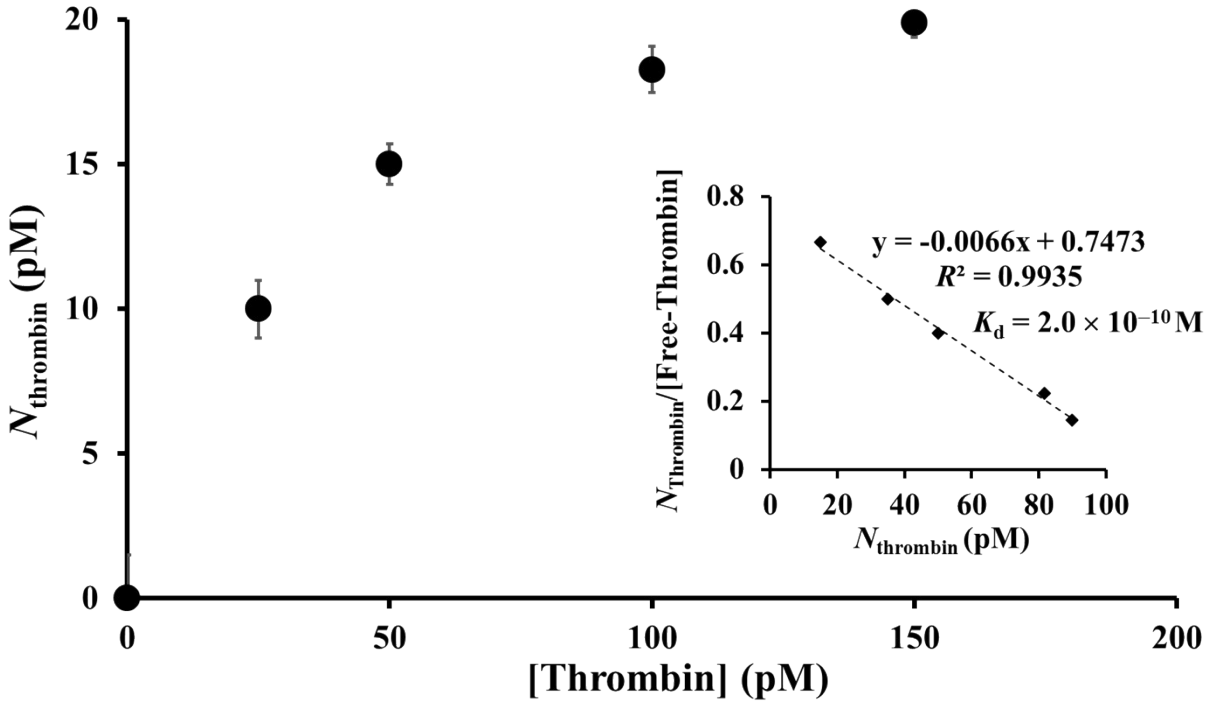

Figure S4. Plot of $N_{Thrombin}$ vs $N_{Thrombin}$/[Free-Thrombin] for calculating the dissociation constant, K_d, for thrombin and GO in the presence of 100 μM BSA. $N_{Thrombin}$ is the concentration of thrombin bound to GO at equilibrium, and [Free-Thrombin] is the free thrombin concentration at equilibrium. Error bars represent the standard deviations of experiments in triplicate.

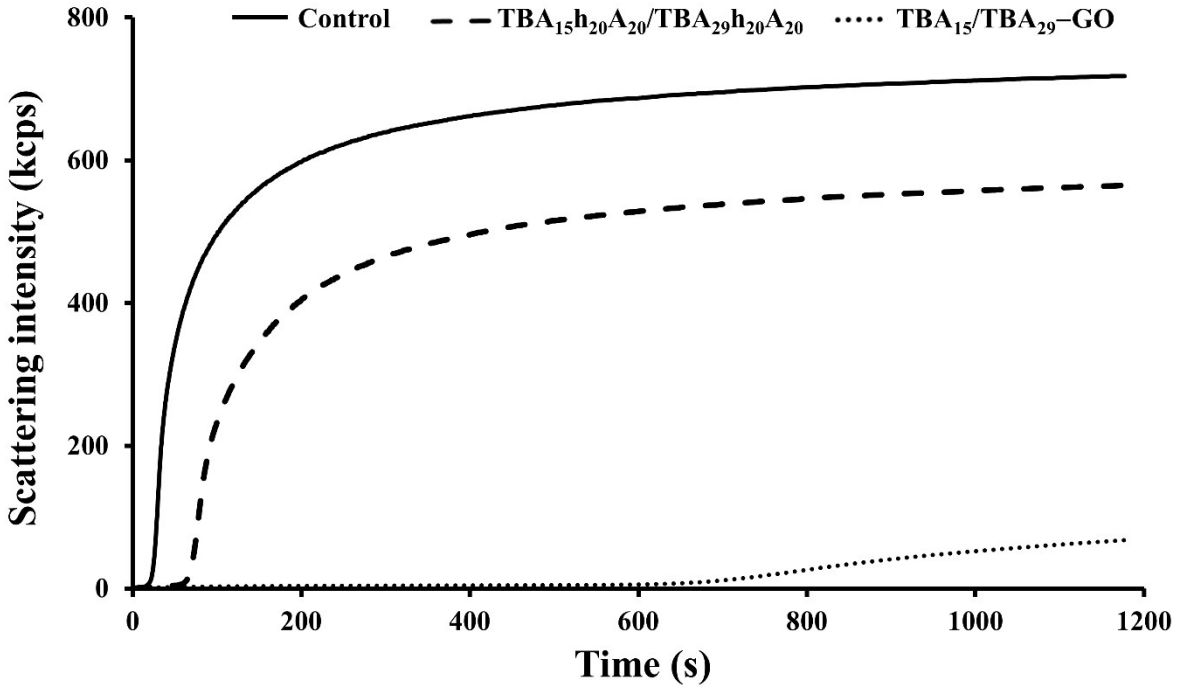

Figure S5. Scattering light intensity as a function of time for $TBA_{15}h_{20}A_{20}/TBA_{29}h_{20}A_{20}$ hybrids (100 nM) and TBA_{15}/TBA_{29}–GO conjugates ($[TBA_{15}h_{20}A_{20}/TBA_{29}h_{20}A_{20}]$ = 100 nM) in human plasma samples. The TCT was the point at which the scattering signal was halfway between the lowest and highest values. The anticoagulation efficiency of the inhibitors was assessed based on the TCT value.

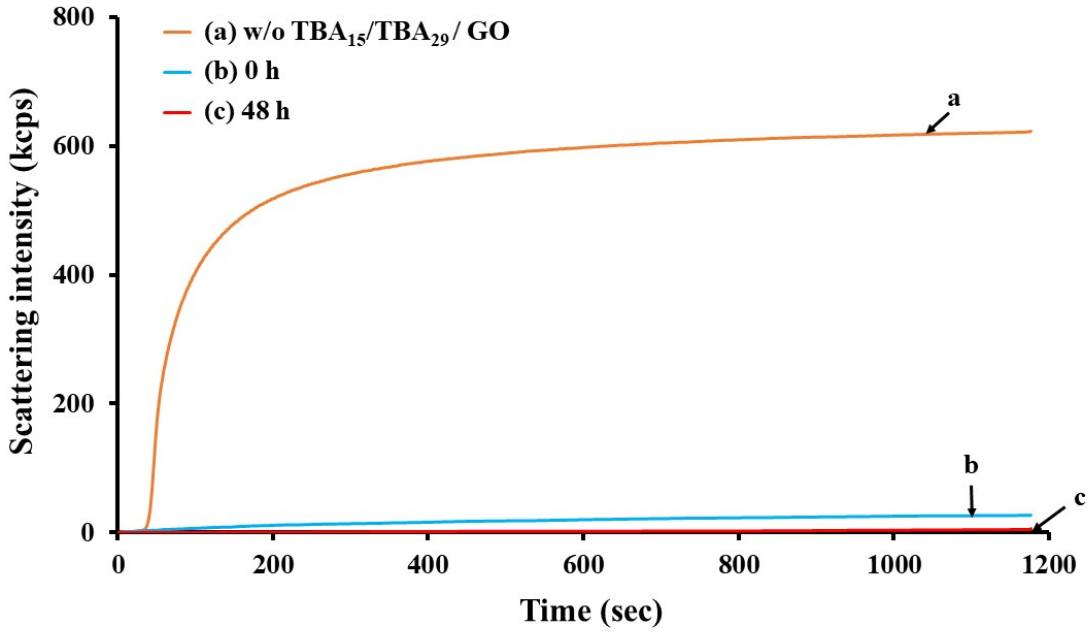

Figure S6. Scattering light intensity as a function of time for the use of TBA_{15}/TBA_{29}–GO as a stable anticoagulant in a representative human plasma sample. TBA_{15}/TBA_{29}–GO ($[TBA_{15}h_{20}A_{20}/TBA_{29}h_{20}A_{20}]$ = 200 nM) was incubated in a 2-fold diluted human plasma sample for 0 h or 48 h, and then, thrombin (15 nM) was added. Other conditions were the same as those described in Figure 2. Curve (a) represents the TCT measurement for human plasma in the absence of TBA_{15}/TBA_{29}–GO as a control. The control experiment confirms that the thrombin-containing plasma is quickly coagulated (TCT~25 s) in the absence of TBA_{15}/TBA_{29}–GO.

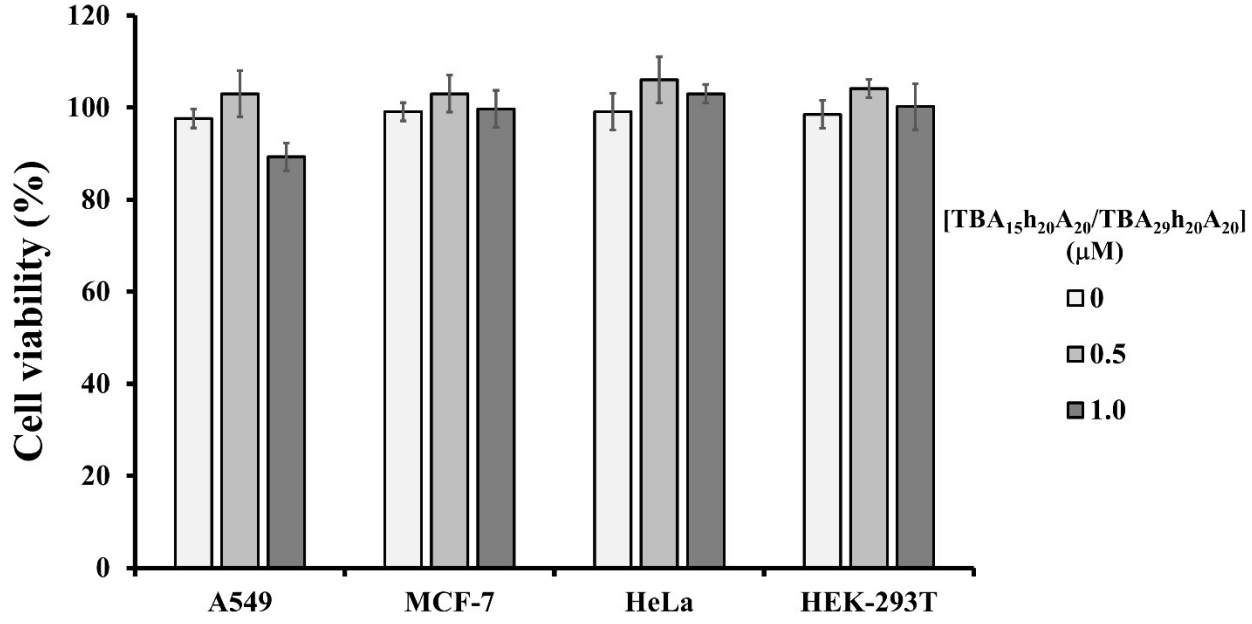

Figure S7. Cell viability of A549, MCF-7, HeLa, and HEK-293T cells (1.0×10^4 cells per well) after treatment with TBA_{15}/TBA_{29}–GO ($[TBA_{15}h_{20}A_{20}/TBA_{29}h_{20}A_{20}]$ = 0–1.0 μM) in the culture media at 37 °C for 24 h. Error bars represent the standard deviation of three repeated measurements.

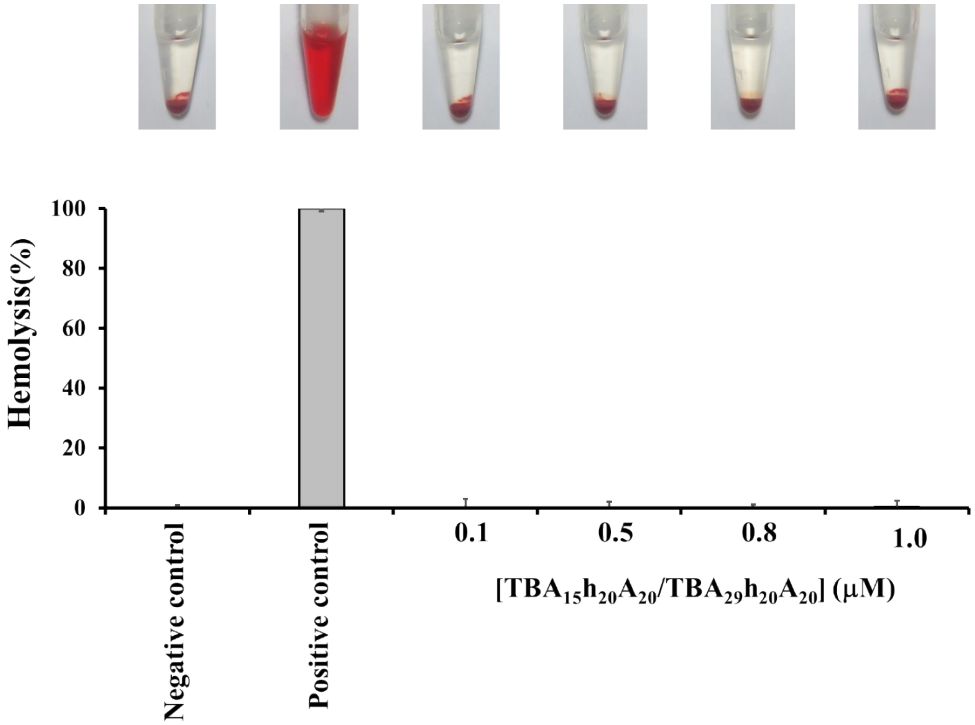

Figure S8. Hemolytic activities of TBA_{15}/TBA_{29}–GO ($[TBA_{15}h_{20}A_{20}/TBA_{29}h_{20}A_{20}]$ = 0.1–1.0 μM) on RBCs. Hemolysis assays with physiological buffer and DI water were used as negative controls and positive controls, respectively. Upper panel: photographs of the corresponding RBC solutions. Error bars represent the standard deviation of three repeated measurements.

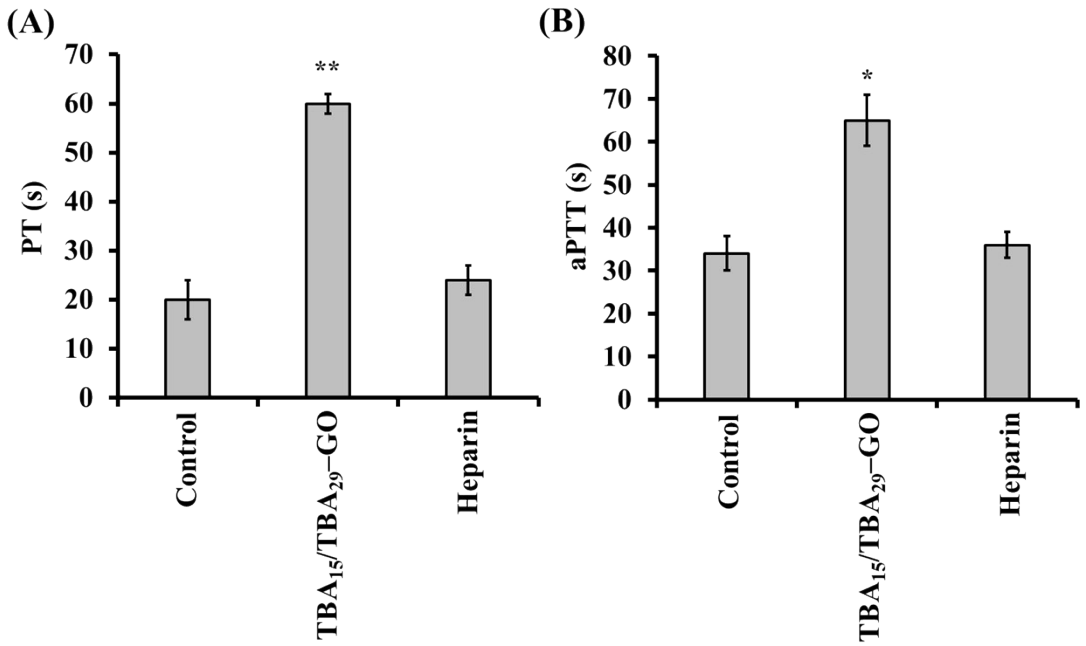

Figure S9. *Ex vivo* (A) PT and (B) aPTT of the TBA_{15}/TBA_{29}–GO conjugates and heparin. TBA_{15}/TBA_{29}–GO conjugates [$TBA_{15}h_{20}A_{20}/TBA_{29}h_{20}A_{20}$] = 10 μM, 200 μL) or heparin (10 μM, 200 μL) inhibitors were administered *via* intravenous injection 30 min before the plasma sample collection. The rats that received only physiological buffer (200 μL) served as a control group. Error bars represent the standard deviation of five rat measurements. Asterisks indicate statistically significant differences (*$p < 0.05$, **$p < 0.01$; $n = 5$) from the control group.